SPR Based Optical Fiber Refractive Index Sensor Using Silver Nanowire Assisted CSMFC

Akhilesh Kumar Pathak and Vinod Kumar Singh

***Abstract*— In this article, a highly sensitive surface plasmon resonance (SPR) based concave shaped refractive index sensor (CSRIS) is designed and analyzed using silver (Ag) nanowire. The SPR effect between the surface plasmon polariton (SPP) and core guided modes of the concave shape (CS) designed sensor is used to measure the variation in refractive index (RI) of analytes (n_a). The sensing performance and the coupling properties of proposed sensor are numerically analyzed using finite element method (FEM) based on COMSOL Multiphysics. Results exhibit a high wavelength and amplitude sensitivity of 9314.28 nm/RIU and 1494 RIU^{-1}, respectively for the RI varying between 1.33 to 1.38 with the resolution of 1.073×10^{-5} RIU. The designed sensor is easy to fabricate as it requires the Ag nanowire to be deposited on the concave shaped microfluidic channel (CSMFC) which is later covered with measurand. various structural parameters, i.e. distance of channel from core, diameter of Ag nanowire, and channel size, are also optimized for better sensing response.**

***Index Terms*— Concave shaped, surface plasmon resonance, nanowire, refractive index, microfluidic.**

I. Introduction

SPR is one of the most promising techniques for the detection of RI of liquid, chemical and gaseous medium. This technique refers to the resonant oscillation of conduction electron at metal-dielectric interface in presence of p-polarized light radiation. The sensor based on SPR phenomenon plays the most important role in detection and monitoring of food safety, various disease, environmental pollution, medical treatment, etc. Various kinds of SPR sensor based on slot, prism, and V-grove configuration have been fabricated in past years. However, such kind of conventional sensors suffer many drawbacks e.g. complex structures, expensive and bulky size. From several years, there has been great attempt to adapt and optimize the traditional bulky technique to optical fiber-based SPR.

The first SPR based optical fiber sensor is proposed and developed by Jorgenson in 1993 in which the cladding of optical fiber is removed from the middle section of fiber and a thin gold film is deposited on the uncladded region to excite SPR [1]. The reported sensor possesses simple fabrication technique and all fiber miniaturization. Since then, large no of SPR based optical fiber sensors have been reported till date e.g. D-shaped polished fiber, tapered fiber structure, fiber Bragg grating, photonic crystal fiber [2]–[4], etc. Out of above-reported sensors, the D-shaped fiber sensors become more attractive among researchers due to its high sensitivity, easy to fabricate, less fragile and practically possible to implement in any hazardous media. In the reported sensing structures, gold (Au) and silver films are used widely in various sensing applications due to their strong absorption. Ag layer always exhibits a high sensitivity and sharper resonance peak in comparison to Au layer which leads to high detection accuracy [5]. In past decades, the metallic nanowire/nanocolumn attracts huge attention of researchers as a good plasmonic medium, in the development of sensors for various applications. In such kind of sensors, the formation of plasmonic modes take place around the nanowire and the resonance peak gets excited when the core guided mode couples with highly lossy plasmonic mode at a particular wavelength which is known as resonance wavelength. There are many sensors developed by using metallic nanowire mostly for temperature sensing [6], [7]. However, the reported sensors show good sensitivity but the main challenges of complexity in fabrication and filling hole with nanowire and selective analytes still persist.

In order to design simple sensing configuration with a high sensitivity, we present a novel design of SPR based optical fiber sensor using CSMFC assisted with Ag nanowire. The designed sensor is based on wavelength interrogation technique which uses the confinement loss to optimize the structural parameters and systematically study sensing response. The numerically simulated results exhibit a high sensitivity of 9314.28 nm/RIU for a wide range of analytes (n_a) varying from 1.33-1.38.

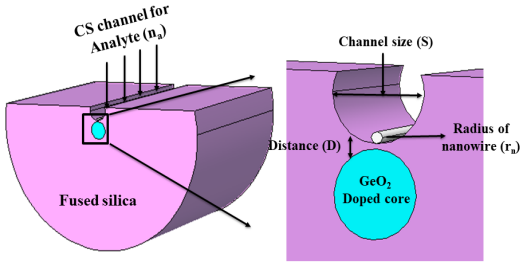

Fig. 1. Cross-sectional view of the proposed sensor design.

II. Structural Design and Numerical Analysis

Figure 1 illustrates the cross-sectional view of the proposed sensor. The sensor is designed using standard single-mode fiber (core/cladding diameter ~9/125 μm) in which CSMFC is incorporated just above the core. The RI of GeO_2 doped silica

Manuscript received November 7, 2019; accepted February 23, 2020. Date of publication March 12, 2020; date of current version March 20, 2020. This work was supported in part by the City, University of London and in part by the EM Leader's Exchange Fellowship Program. *(Corresponding authors: Akhilesh Kumar Pathak; Vinod Kumar Singh.)*

The authors are with the Optical Fiber Laboratory, Indian Institute of Technology (Indian School of Mines) at Dhanbad, Dhanbad 826004, India (e-mail: akhileshpathak57@ap.ism.ac.in; vksingh@iitism.ac.in).

This article has supplementary downloadable material available at http://ieeexplore.ieee.org, provided by the author.

Color versions of one or more of the figures in this letter are available online at http://ieeexplore.ieee.org.

Digital Object Identifier 10.1109/LPT.2020.2980470

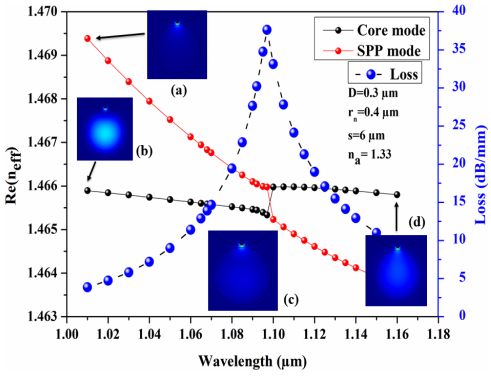

Fig. 2. Dispersion curve of the proposed sensor for core and SPP modes at $n_a = 1.33$.

core and fused silica cladding are calculated by the following Sellmeier equation [8].

$$n^2(\lambda^2) = 1 + \frac{B_1\lambda^2}{\lambda^2 - C_1} + \frac{B_2\lambda^2}{\lambda^2 - C_2} + \frac{B_3\lambda^2}{\lambda^2 - C_3} \quad (1)$$

where $B_{1,2,3}$ and $C_{1,2,3}$, represent Sellimeiers coefficients whose values are taken from previous article. The material dispersion of Ag nanowire is calculated by Lorentz-Drude model, as it gives more accurate prediction of permittivity and closer to the experimental values and can be defined as [9], [10]

$$\varepsilon_m = 1 - \frac{\Omega_p^2}{\omega(\omega - i\Gamma_0)} + \sum_{j=1}^{k} \frac{f_j\omega_p^2}{(\omega_j^2 - \omega^2) + j\omega\Gamma_i} \quad (2)$$

where, ε_m and ω_p represent the dielectric constant and the plasma frequency whereas k is the number of oscillators with frequency ω_p and strength f_j, while Ωp, which is $\sqrt{(f_0 .\omega_p)}$, shows the plasma frequency related with intraband transition.

The distance (D) and size (s) of CSMFC are initially considered to be 0.5 μm and 5 μm, respectively just above the core. Later the MFC is filled with analytes of RI = 1.33 along with Ag nanowire of radius (r_n) 0.5 μm that sinks to the bottom of channel due to gravity. The designed sensor is characterized and analyzed using full vectorial FEM based on COMSOL Multiphysics [11]. The modal analysis is performed in XY plane while the propagation of light is considered in Z direction.

A microchannel can be easily fabricated at the polished D shaped edge near the core of optical fiber by considering a gaussian field distribution. Due to small sized channel a very small amount of aqueous solution is required for detection. The Gaussian field distribution is positioned at the edge of polished surface and the part of area exposed to the field is removed to form the sensing structure as shown in Fig.1. The profile of field distribution can be written in the form of following equation [12]

$$y = y_0 + Ae^{-\frac{(x-x_c)^2}{2\omega^2}} \quad (3)$$

where y_0, x_c, ω and A represent offset, center, width and amplitude respectively. Later the Ag nanowire can be deposited by using colloidal solution of Ag inside the CS channel as reported by Yang *et al.* [13].

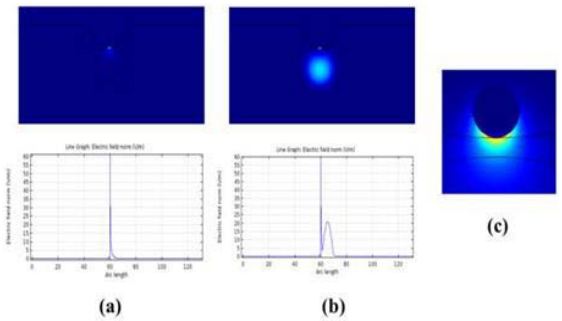

Fig. 3. Electric field distribution of proposed sensor for (a) SPP mode along with vertical field plot (b). Core mode along with vertical field plot, and (c) field distribution around nanowire [15].

III. Results and Discussion

Figure 2 illustrates the dispersion relation curve between core guided and SPP modes. The plot indicates the real effective index ($Re(n_{eff})$) of core and SPP modes at various wavelengths along with the modal loss spectra of the designed sensor. From Fig.1 we can observe that the $Re(n_{eff})$ of SPP mode (shown by red dotted line) decreases linearly while $Re(n_{eff})$ of core mode (shown by black dotted line) remains constant throughout the wavelength variation. The blue dotted line illustrates the model loss spectra of designed sensor at n_a =1.33. The modal loss of proposed sensor is calculated by using imaginary part of effective index from following relation [14]

$$\alpha(\text{dB/m}) = 8.686.\, k_0.\, \text{Im}\,(n_{eff}) \quad (4)$$

where the wavenumber (k_0) can be defined as $k_0 = 2\pi/\lambda$.

The plasmonic mode is very lossy in comparison to the core guided mode. The inset (a) and (b) in figure 2 illustrate the field distribution in SPP mode and core mode respectively at $\lambda = 1.01$ μm in which the maximum energy distribution in core mode may be observed clearly. With increase in wavelength, the energy transfer from core mode to plasmonic modes takes place at resonance wavelength (λ_R) = 1.097 μm. The n_{eff} of two modes become similar which is known as phase matching or resonance condition. At this λ_R the energy gets completely transferred from core mode to plasmonic mode and form supermodes which gives maximum loss of 37.61 dB/mm. The phase match field profile is shown in inset (c). The inset (d) shows the field distribution in core region at non resonance wavelength.

Figure 3 (a) and (b) illustrate the Hx field contour along with their Hx field variation with respect to y-axis for the SPP and core mode, respectively at $n_a = 1.33$. Figure 3(c) shows the electric field distribution around Ag nanowire. The Hx field distribution for SPP mode is shown on the top of Fig. 3(a). From the plot, we can clearly observe that this mode is localized around Ag nanowire while its variation along y-axis is shown on its bottom in Fig.3(a). The field variation clearly exhibits the plasmonic peak at metal-dielectric interface and decay exponentially. Figure 3(b) shows the mode coupling of SPP mode with core-guided mode. The decent Hx field value in the core can be clearly observed on the top of Fig. 3(b) whereas the its field distribution is shown on the bottom of Fig. 3(b) which exhibits the coupled supermode profile. Figure 3(c) shows the mode field pattern around the Ag nanowire

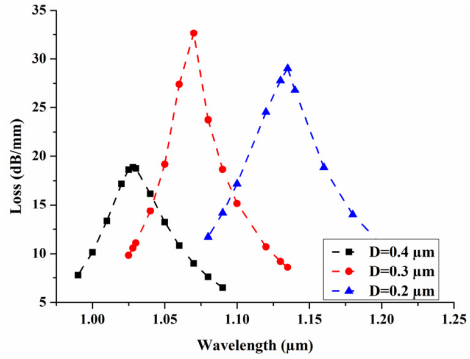

Fig. 4. Confinement modal loss spectra with the variation of MFC distance (D).

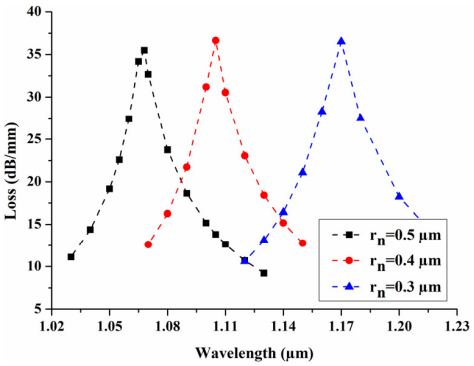

Fig. 5. Confinement modal loss spectra with the variation of nanowire radius.

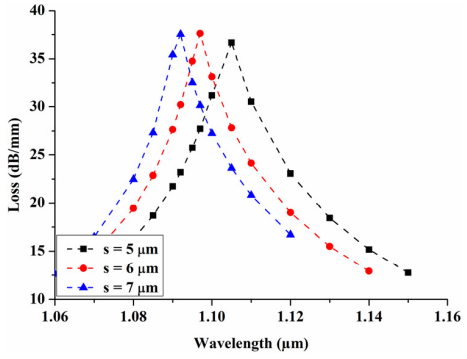

Fig. 6. Confinement modal loss spectra with the variation of channel size (s).

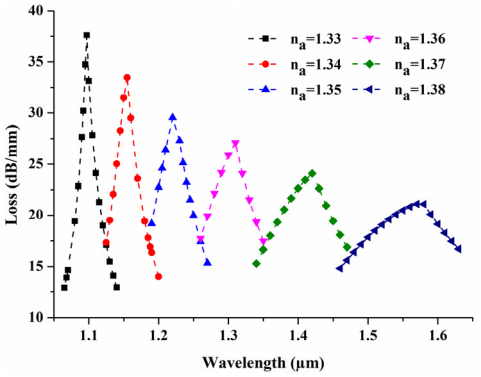

Fig. 7. Confinement modal loss spectra with analytes of varying RI (n_a).

Before starting the characterization of the designed sensor, all structural parameters (D, r_n, and s) must be optimized to achieve a high sensitivity. In the numerical simulation, the distance of the CS channel from the core plays the significant role in achieving the maximum coupling of core and SPP modes. While the investigation carried out for D, other parameters like r_n, s and n_a are kept constant. Figure 4 illustrates the confinement loss spectra of the fundamental mode corresponding to the variation of MFC distance from the core. We can clearly observe from the figure that when the distance of MFC varies from 0.2 μm to 0.4 μm, the loss first increases and then experience a sudden decrement with an evident red shift in loss spectra. From plot, we may see that the maximum modal loss of 32.65 dB/mm is obtained for D = 0.3 μm at λ_R = 1.07 μm while 29.03 dB/mm and 18.86 dB/mm for 0.2 μm and 0.4 μm respectively. Hence, we have considered D = 0.3 μm as the optimized separation of CSMFC from the core.

Figure 5 shows the loss spectra of the fundamental mode for various radius (r_n) of Ag nanowire. From Fig. 5, we can observe a strong influence of radius of nanowire (r_n) over the sensing performance. Before the optimization of rn, all other parameters are kept constant and rn is varied as 0.3 μm, 0.4 μm, and 0.5 μm. The maximum modal loss of 36.52 dB/mm, 36.65 dB/mm, and 35.50 dB/mm are obtained for 0.3 μm, 0.4 μm, and 0.5 μm of r_n respectively with redshift in loss spectra. Hence optimized r_n is considered as 0.4 μm because of its maximum modal loss out of three values for optimized D = 0.3 μm.

The size of CSMFC also plays an important role in the sensing performance. In order to investigate the influence of channel size (s) on the performance of designed sensor, we keep the distance of CSMFC from the core fixed while the channel size is varied from 5 μm to 7 μm with interval of 1 μm. The confinement loss spectra of fundamental mode with the variation of s is shown in Fig. 6. It is clearly observed from Fig.6, that when the size of channel increases from 5 μm to 7 μm, the value of loss peak wavelength declines from 1.105 μm to 1.092 μm, which illustrates a strong red shift with maximum modal loss of 37.61 dB/mm obtained for s = 6 μm.

After optimization of all structural parameters, the designed sensor is characterized for a wide range of RI varying from 1.33 to 1.38. The variation in confinement loss spectra with respect to wavelength for various n_a is shown in Fig.7. Figure 7 exhibits a strong blue shift in confinement loss spectra, varying from λ_R = 1.097 μm to 1.570 μm when the n_a changes from 1.33 to 1.38. Here, we can interpret that full width and half maxima (FWHM) of resonance peak getting broaden with increasing the measurand refractive indices. The broadening of these peaks arises due to the comparative lower index contrast because of increase of n_a.

Figure 8 illustrates the variation in resonance wavelength with respect to corresponding analytes. The simulated data points are obtained from Fig. 7. From Fig. 8 we can clearly observe a very good linear relationship between λ_R and n_a, with a good linearity (R^2 = 0.9646) for the sensing range n_a = 1.33 to 1.38. The sensitivity of the designed sensor is calculated by wavelength interrogation technique using following equation [14]

$$S_\lambda = \Delta\lambda_{peak}/\Delta n_a (\text{nm/RIU}) \quad (5)$$

where, S_λ and $\Delta\lambda_{peak}$ are the sensitivity and shift in resonance wavelength respectively. Δn_a represents the change in RI of analytes.

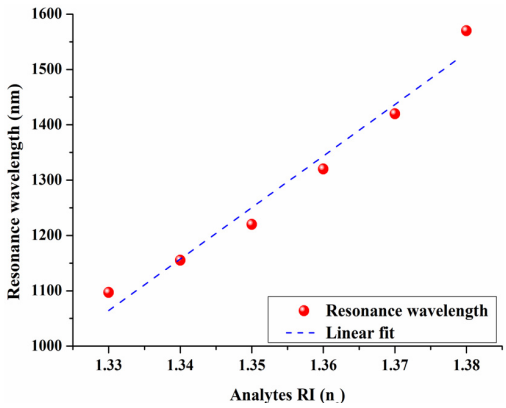

Fig. 8. Sensitivity plot for designed sensor.

TABLE I
THE DETAILED COMPARISON OF VARIOUS SENSORS AND THEIR SENSITIVITY

Previous works	Sensitivity (nm/RIU)
Ref. [16]	4391
Ref. [17]	5700
Ref. [18]	8860.93
Present work	9314.28

The designed sensor shows a high sensitivity of 9314.28 nm/RIU. The resonance wavelength of designed sensor is obtained of 1.097 μm, 1.115 μm, 1.220 μm, 1.320 μm, 1.420 μm, and 1.570 μm corresponding to n_a = 1.33, 1.34, 1.35, 1.36, 1.37, and 1.38, respectively. In addition to its high sensitivity, the main novelty of the proposed sensor is its design. Here we have incorporated a CSMFC just above the core to enhance the sensitivity and minimize the wastage of analytes, as it requires only a small amount of measurand to be detected. Moreover, the designed sensor is easy to fabricate and implement, in contrast to the photonic crystal fiber (PCF) sensors due to its external metal-coated structures.

Table.I represents the detailed comparison of the sensitivity of proposed work with other reported work.

The resolution of designed sensor is also calculated for better understanding. The resolution of the sensor is defined by the following relation [14]

$$R = \Delta n_a . (\Delta\lambda_{min}/\Delta\lambda_{peak})\, RIU \quad (6)$$

where $\Delta\lambda_{min}$ is the minimum spectral resolution and is considered as 0.1 nm. Then the resolution of designed sensor is estimated to be 1.073×10^{-5} RIU which exhibits that the designed sensor is capable in detecting a small change in n_a of the order of 10^{-5}. Tolerance on fabrication is also investigated in the present work with ± 2 % variation of structural parameter and obtained a small variation in sensitivity with respect to its optimum value.

IV. CONCLUSION

In summary, we have proposed a novel SPR based concave shaped refractive index sensor for a wide range of RI sensing. The sensing performance and the optimization of structural parameters of the designed sensor are numerically investigated by using FEM technique. The theoretical results obtained by numerical simulations exhibit a high wavelength and amplitude sensitivity of 9314.28 nm/RIU and 1494 RIU^{-1} for a wide range of RI varying from 1.33 to 1.38 and exhibits a high resolution of 1.073×10^{-5} RIU. The impact of variation and optimization of structural parameters are also studied here. From the investigation, we came to know that the D, r_n, and s of CSRIS are the key factors to achieve a high sensitivity. The sensing response of the designed sensor illustrates that the designed sensor can be used in various chemical and biological sensing and its novel shape can be utilized for further improvement to achieve more sensitivity.

ACKNOWLEDGMENT

The work is carried out in IIT (ISM), Dhanbad with the collaborative support of the City, University of London, under EM Leader's exchange program.

REFERENCES

[1] R. C. Jorgenson and S. S. Yee, "A fiber-optic chemical sensor based on surface plasmon resonance," *Sens. Actuators B, Chem.*, vol. 12, no. 3, pp. 213–220, Apr. 1993.
[2] Y. Ying, G.-Y. Si, F.-J. Luan, K. Xu, Y.-W. Qi, and H.-N. Li, "Recent research progress of optical fiber sensors based on D-shaped structure," *Opt. Laser Technol.*, vol. 90, pp. 149–157, May 2017.
[3] Y.-C. Kim, W. Peng, S. Banerji, and K. S. Booksh, "Tapered fiber optic surface plasmon resonance sensor for analyses of vapor and liquid phases," *Opt. Lett.*, vol. 30, no. 17, p. 2218, Sep. 2005.
[4] C. Liu *et al.*, "Birefringent PCF-based SPR sensor for a broad range of low refractive index detection," *IEEE Photon. Technol. Lett.*, vol. 30, no. 16, pp. 1471–1474, Aug. 15, 2018.
[5] M. Mitsushio, K. Miyashita, and M. Higo, "Sensor properties and surface characterization of the metal-deposited SPR optical fiber sensors with Au, Ag, Cu, and Al," *Sens. Actuators A, Phys.*, vol. 125, no. 2, pp. 296–303, Jan. 2006.
[6] X. Yang, Y. Lu, L. Duan, B. Liu, and J. Yao, "Temperature sensor based on hollow fiber filled with graphene-ag composite nanowire and liquid," *Plasmonics*, vol. 12, no. 6, pp. 1805–1811, Dec. 2017.
[7] N. Luan, R. Wang, W. Lv, Y. Lu, and J. Yao, "Surface plasmon resonance temperature sensor based on photonic crystal fibers randomly filled with silver nanowires," *Sensors*, vol. 14, no. 9, pp. 16035–16045, 2014.
[8] A. K. Pathak, B. M. A. Rahman, V. K. Singh, and S. Kumari, "Sensitivity enhancement of a concave shaped optical fiber refractive index sensor covered with multiple au nanowires," *Sensors*, vol. 19, no. 19, p. 4210, Sep. 2019.
[9] A. D. Rakić, AB Djurišić, J. M. Elazar, and M. L. Majewski, "Optical properties of metallic films for vertical-cavity optoelectronic devices," *Appl. Opt.*, vol. 37, no. 22, p. 5271, Aug. 1998.
[10] D. Li and G. Zhou, "Theoretical simulation of a novel birefringent photonic crystal fiber with surface plasmon resonance around 1300 nm," *Chin. Phys. B*, vol. 25, no. 3, Mar. 2016, Art. no. 034209.
[11] B. M. A. Rahman and J. B. Davies, "Finite-element analysis of optical and microwave waveguide problems," *IEEE Trans. Microw. Theory Techn.*, vol. 32, no. 1, pp. 20–28, Jan. 1984.
[12] J. N. Dash, R. Das, and R. Jha, "AZO coated microchannel incorporated PCF-based SPR sensor: A numerical analysis," *IEEE Photon. Technol. Lett.*, vol. 30, no. 11, pp. 1032–1035, Jun. 1, 2018.
[13] X. Yang, Y. Lu, L. Duan, H. Zhang, and J. Yao, "Photonic crystal fiber temperature sensor filled with liquid and silver nanowires," *Proc. SPIE*, vol. 10872, Feb. 2019, Art. no. 108720V.
[14] A. K. Pathak, S. Ghosh, R. K. Gangwar, B. M. A. Rahman, and V. K. Singh, "Metal nanowire assisted hollow core fiber sensor for an efficient detection of small refractive index change of measurand liquid," *Plasmonics*, vol. 14, no. 6, pp. 1823–1830, Dec. 2019.
[15] Q. Li and M. Qiu, "Plasmonic wave propagation in silver nanowires: Guiding modes or not?" *Opt. Express*, vol. 21, no. 7, p. 8587, Apr. 2013.
[16] G. An *et al.*, "Ultra-stable D-shaped optical fiber refractive index sensor with graphene-gold deposited platform," *Plasmonics*, vol. 14, no. 1, pp. 155–163, Feb. 2019.
[17] A. Patnaik, K. Senthilnathan, and R. Jha, "Graphene-based conducting metal oxide coated D-Shaped optical fiber SPR sensor," *IEEE Photon. Technol. Lett.*, vol. 27, no. 23, pp. 2437–2440, Dec. 1, 2015.
[18] H. Fu *et al.*, "A high sensitivity D-type surface plasmon resonance optical fiber refractive index sensor with graphene coated silver nanocolumns," *Opt. Fiber Technol.*, vol. 48, pp. 34–39, Mar. 2019.